Published in "Diabetes 55: 2286-2293, 2006"
which should be cited to refer to this work.

Altered Skeletal Muscle Subsarcolemmal Mitochondrial Compartment During Catch-Up Fat After Caloric Restriction

Raffaella Crescenzo,[1] Lillà Lionetti,[1] Maria Pina Mollica,[1] Marialuisa Ferraro,[1] Elvira D'Andrea,[1] Davide Mainieri,[2] Abdul G. Dulloo,[2] Giovanna Liverini,[1] and Susanna Iossa[1]

An accelerated rate of fat recovery (catch-up fat) and insulin resistance are characteristic features of weight recovery after caloric restriction, with implications for the pathophysiology of catch-up growth and weight fluctuations. Using a previously described rat model of weight recovery in which catch-up fat and skeletal muscle insulin resistance have been linked to suppressed thermogenesis per se, we investigated alterations in mitochondrial energetics and oxidative stress in subsarcolemmal (SS) and intermyofibrillar (IMF) skeletal muscle mitochondria. After 2 weeks of semistarvation followed by 1 week of refeeding, the refed rats show persistent and selective reductions in SS mitochondrial mass (assessed from citrate synthase activity in tissue homogenate and isolated mitochondria) and oxidative capacity. Furthermore, the refed rats show, in both SS and IMF muscle mitochondria, a lower aconitase activity (whose inactivation is an index of increased reactive oxygen species [ROS]), associated with higher superoxide dismutase activity and increased proton leak. Taken together, these studies suggest that diminished skeletal muscle mitochondrial mass and function, specifically in the SS mitochondrial compartment, contribute to the high metabolic efficiency for catch-up fat after caloric restriction and underscore a potential link between diminished skeletal muscle SS mitochondrial energetics, increased ROS concentration, and insulin resistance during catch-up fat. *Diabetes* 55:2286–2293, 2006

In response to diminished food supply, humans and other mammals can elicit a reduction in energy expenditure, which is partly attributed to an increased metabolic efficiency (1,2). This is viewed as an adaptive response to food scarcity because it slows the rate of weight loss or reduces the energy cost for weight maintenance. Because suppressed thermogenesis also persists for some time upon refeeding (1,3–9) and the energy spared is directed specifically at accelerating recovery of body fat (or catch-up fat) (8), it can also be viewed as the outcome of a control system that operates as a feedback loop between depletion/repletion of the fat stores and suppressed thermogenesis (10). This energy conservation mechanism, which probably evolved to optimize survival capacity in a lifestyle characterized by periodic food shortage, is an important factor that nowadays contributes to the relapse of obesity after slimming and hence to the poor efficacy of dietary restriction in the management of obesity. It is also a contributing factor to the high rate of fat deposition that characterizes catch-up growth after earlier growth retardation (10) and has been implicated in the link between early malnutrition, catch-up growth, and increased risks for type 2 diabetes and cardiovascular disease later in life (11).

Using a validated rat model of weight recovery in which catch-up fat results from suppressed thermogenesis per se (8,10), it was recently shown that in response to a glucose load, plasma insulin concentrations are higher in the refed animals than in controls, even at a time point when body fat in the refed animals had not yet exceeded that of controls (12). Furthermore, the use of euglycemic-hyperinsulinemic clamp revealed that in vivo insulin-stimulated glucose utilization is lower in skeletal muscles from refed than in those from control animals (13). Because skeletal muscle is an important contributor to whole-body energy expenditure and a major site for insulin-stimulated glucose disposal, the possibility arises that suppressed thermogenesis in this tissue would result in a reduction in glucose utilization, thereby leading to compensatory hyperinsulinemia. This in turn would serve to redirect the spared glucose toward storage as lipids in adipose tissue and hence would account for the catch-up fat phenomenon.

Within the context of this hypothesis that skeletal muscle is an important effector site for suppressed thermogenesis favoring catch-up fat, we report here studies that examined the extent to which alterations in mitochondrial energetics in this tissue might contribute to the high metabolic efficiency associated with catch-up fat and insulin resistance.

RESEARCH DESIGN AND METHODS

Male Sprague Dawley rats, aged 6 weeks, were adapted to room and cage environments for at least 5 days before the start of experiments. They were caged singly in a temperature-controlled room (22 ± 1°C) with a 12-h light/dark cycle, maintained on a commercial pelleted chow diet (Mucedola, Settimo Milanese, Italy) with free access to water. Animals used in the present studies were maintained in accordance with the guidelines of Italian Health Ministry. Experiments described here used a validated rat model for studying adjustments in energy expenditure during refeeding (8,10). The cardinal

From the [1]Department of Biological Sciences, Section of Physiology, University of Naples, Naples, Italy; and the [2]Department of Medicine, Division of Physiology, University of Fribourg, Fribourg, Switzerland.

Address correspondence and reprint requests to Susanna Iossa, Dipartimento delle Scienze Biologiche, Sezione di Fisiologia, Via Mezzocannone 8, I-80134, Napoli, Italy. E-mail: susiossa@unina.it.

HOMA, homeostasis model assessment; IMF, intermyofibrillar; NEFA, nonesterified fatty acid; ROS, reactive oxygen species; SOD, superoxide dismutase; SS, subsarcolemmal; UCP3, uncoupling protein 3.

DOI: 10.2337/db06-0312

feature of this design is that after 2 weeks of caloric restriction, the growth-arrested animals are refed at the same level of energy intake as that of weight-matched controls, i.e., the crucial comparison is therefore between refed animals regaining weight versus spontaneously growing controls that are matched for weight at the onset of the refeeding period. Under these conditions, the refed animals show increased rate of body fat gain due to lower energy expenditure than controls. To eliminate the impact of an elevated fat mass per se on the measured parameters in blood and skeletal muscle, the latter were collected/harvested at the end of the 1st week of refeeding, i.e., at time points during refeeding when body fat in refed animals had not yet exceeded that of controls. More specifically, rats selected on the basis of body weight being within ±5 g mean body wt were food restricted for 2 weeks at ~50% of their spontaneous chow intake, and at the end of this semistarvation period (corresponding to day 0 of refeeding), one-half of semistarved rats and one-half of control rats were killed by decapitation for measurements of body composition or for blood collection and skeletal muscle harvesting. The other half of semistarved rats were refed the chow diet at a level approximately equal in metabolizable energy content to the spontaneous food intake of weight-matched controls. The refed groups therefore consumed, on a day-to-day basis, the same amount of food energy as controls fed ad libitum. At the end of a 1-week period of controlled refeeding, animals in both refed and control groups were killed by decapitation for measurements of body composition and energy balance or for blood collection and skeletal muscle harvesting.

Energy balance measurements were conducted by the comparative carcass technique over 2 weeks of food restriction and 1 week of refeeding, during which metabolizable energy intake was monitored, as detailed previously (14). Energy expenditure was determined as the difference between energy gain and metabolizable energy intake, and net energy expenditure was calculated from energy expenditure excluding the total cost of storage. The total cost of storage was determined by using the values of 1.25 and 0.36 kJ/kJ for energy loss in storing protein and fat, respectively (14).

Isolation of skeletal muscle mitochondria and assay of uncoupling protein 3. Hind leg muscles were rapidly removed and used for the preparation of subsarcolemmal (SS) and intermyofibrillar (IMF) mitochondria, as described previously (14). Immediately after the isolation, aliquots of mitochondria were frozen and stored at −80°C for the determination of uncoupling protein 3 (UCP3) by Western blotting using UCP3 antibody (Chemicon International, Temecula, CA), as previously described (15,16).

Measurements of mitochondrial respiration and basal and palmitate-induced proton leak. Oxygen consumption was measured polarographically with a Clark-type electrode (Yellow Springs Instruments, Yellow Springs, OH) at 30°C, using a medium containing 30 mmol/l KCl, 6 mmol/l $MgCl_2$, 75 mmol/l sucrose, 1 mmol/l EDTA, 20 mmol/l KH_2PO_4, pH 7.0, and 0.1% (wt/vol) fatty acid-free BSA. In the presence of 0.6 mmol/l ADP, state 3 oxygen consumption was measured. State 4 was obtained in the absence of ADP. Respiratory substrates used were 10 mmol/l succinate and 3.75 μmol/l rotenone; 10 mmol/l glutamate and 2.5 mmol/l malate; and 40 μmol/l palmitoyl CoA, 2 mmol/l carnitine, and 2.5 mmol/l malate.

Mitochondrial oxygen consumption was measured polarographically, and membrane potential recordings were performed in parallel with safranin O using a Jasco dual-wavelength spectrophotometer (511–533 nm) (17). The absorbance readings were transferred to millivolt membrane potential using the Nernst equation, $D\Psi = 61\ \text{mV} \times \log([K^+]_{in}/[K^+]_{out})$, and calibration curves made for each preparation as previously reported (18). Measurements were carried out at 30°C in a medium containing 30 mmol/l LiCl, 6 mmol/l $MgCl_2$, 75 mmol/l sucrose, 1 mmol/l EDTA, 20 mmol/l Tris-P, pH 7.0, and 0.1% (wt/vol) BSA in the presence of succinate (10 mmol/l), rotenone (3.75 μmol/l), oligomycin (2 μg/ml), safranin O (83.3 nmol/mg), and nigericin (80 ng/ml). Oxygen consumption and membrane potential were titrated by sequential additions of malonate up to 5 mmol/l for SS and 3 mmol/l for IMF mitochondria.

Mitochondrial oxygen consumption and membrane potential were measured as above in the presence of succinate (10 mmol/l), rotenone (3.75 μmol/l), oligomycin (2 μg/ml), safranin O (83.3 nmol/mg), and palmitate (45 μmol/l and 65 μmol/l for SS and IMF mitochondria, respectively). Sequential additions of malonate were up to 1 mmol/l for SS and 625 μmol/l for IMF mitochondria.

Determination of mitochondrial mass. Mitochondrial protein mass was assessed by two approaches, namely *1*) by measuring the activity of a mitochondrial marker enzyme, citrate synthase, in skeletal muscle homogenates and in isolated mitochondria, according to Srere (19), and *2*) by evaluating the mitochondrial yield. In the first approach, citrate synthase activity, measured in the homogenate and expressed per gram wet muscle, reflects the product of mitochondrial protein mass and specific activity of the citrate synthase enzyme. To determine citrate synthase specific activity, measurements were made in isolated SS and IMF mitochondria, and the results were expressed per milligram mitochondrial protein. In addition, to determine protein mass in each mitochondrial subpopulation, citrate synthase activity in IMF and SS mitochondria was expressed per gram starting wet tissue. It should be noted that both IMF and SS mitochondrial preparations were almost pure because we found that their contamination by other ATPase-containing membranes was <10%. In the second approach, in which mitochondrial SS and IMF protein mass was evaluated as mitochondrial protein yield, the milligram of mitochondrial proteins obtained from the isolated SS or IMF mitochondrial subpopulations was expressed per gram starting wet tissue. In principle, changes in mitochondrial yield could result from *1*) changes in the amount of mitochondria in the starting tissue or *2*) changes in the sedimentation characteristics of the organelles. To exclude the possibility that changes in mitochondrial yield could result from loss of mitochondria during the isolation procedure, we also assessed the recovery of citrate synthase activity in the various fractions during the isolation procedure of SS and IMF mitochondria.

Determination of mitochondrial aconitase and superoxide dismutase specific activity. Mitochondria were solubilized in 1% Triton X-100 (40–60 μg for aconitase and 7–9 μg mitochondrial protein for superoxide dismutase [SOD]). Aconitase specific activity was measured in a medium containing 30 mmol/l sodium citrate, 0.6 mmol/l $MnCl_2$, 0.2 mmol/l NADP, 50 mmol/l Tris-HCl, pH 7.4, and 2 units isocitrate dehydrogenase, and the formation of NADPH was followed spectrophotometrically (340 nm) at 25°C (20). SOD specific activity was measured in a medium containing 0.1 mmol/l EDTA, 2 mmol/l KCN, 50 mmol/l KH_2PO_4, pH 7.8, 20 mmol/l cythocrome c, 0.1 mmol/l xanthyne, and 0.01 unit xanthyne oxidase. Determinations were carried out spectrophotometrically (550 nm) at 25°C by monitoring the decrease in the reduction rate of cythocrome c by superoxide radicals generated by the xanthine-xanthine oxidase system. One unit of SOD activity is defined as the concentration of enzyme that inhibits cythocrome c reduction by 50% in the presence of xanthine+xanthine oxidase (21).

Blood parameters. The blood samples were centrifuged at $1{,}400g_{av}$ for 8 min at 4°C. Plasma was removed and stored at −20°C. Plasma insulin concentrations were measured using enzyme-linked immunosorbent assay kits in a single assay to remove interassay variations (Mercodia, Uppsala, Sweden). Plasma glucose and nonesterified fatty acid (NEFA) concentrations were measured by colorimetric enzymatic method using commercial kits (Pokler Italia [Genova, Italy] for glucose; Roche Diagnostics [Mannheim, Germany] for NEFA). Insulin resistance was assessed by homeostasis model assessment (HOMA) index = (glucose [mg/dl] × insulin [mU/l])/405 (22).

Chemicals. All chemicals used were of analytical grade and were purchased from Sigma (St. Louis, MO).

Statistical analysis. Data are provided as means ± SE. Statistical analyses were performed using two-tailed unpaired Student's *t* test or nonlinear regression curve fit. All analyses were performed using GraphPad Prism 4 (GraphPad Software, San Diego, CA).

RESULTS

The data on body composition and metabolic characterization at the end of semistarvation and refeeding are shown in Table 1. At the end of the 2-week period of semistarvation, the food-restricted rats had similar body weight and protein content but significantly lower fat content than controls. In addition, plasma NEFA and glucose concentrations, as well as the HOMA index, were significantly lower in the food-restricted rats than in controls, whereas no difference was found in plasma insulin levels. During the 1-week period of refeeding, the previously food-restricted rats exhibited significantly greater gain in lipid mass than in controls, whereas the gain in body protein and weight were not significantly different. Energy balance data during this refeeding period (Table 1) indicate that, in the absence of significant differences in energy intake between refed and control groups, the greater gain in body fat and energy in the refed animals resulted from lower values of energy expenditure and net energy expenditure (which can represent the cost of body energy maintenance) than in controls. In addition, plasma glucose concentrations and the HOMA index were significantly higher in refed than in control rats, whereas no differences were found in plasma insulin and NEFA levels.

TABLE 1
Body composition, energy balance, and plasma levels of substrates and hormones at the end of semistarvation and after 7 days of refeeding

Semistarvation	Control	Restricted
Body weight (g)	222.2 ± 2.8	222.5 ± 2.1
Body lipids (g)	18.2 ± 1.3	8.7 ± 1.1*
Body proteins (g)	45.7 ± 1.8	47.0 ± 1.2
Body water (g)	145 ± 2.1	155 ± 2.1
Insulin (ng/ml)	1.89 ± 0.47	1.78 ± 0.95
Glucose (mg/dl)	228 ± 12	174 ± 15*
HOMA index	24.8 ± 1.2	17.6 ± 0.9*
NEFA (mmol/l)	0.107 ± 0.012	0.061 ± 0.012*
Refeeding	**Control**	**Refed**
Weight gain (g)	64 ± 4	68 ± 6
Fat gain (g)	11.5 ± 0.7	18.0 ± 0.7*
Protein gain (g)	11.2 ± 2.8	11.0 ± 1.2
Energy gain (kJ)	686 ± 31	945 ± 40*
ME intake (kJ)	2,404 ± 51	2,288 ± 47
Energy expenditure (kJ)	1,718 ± 86	1,343 ± 78*
Gross efficiency (%)	0.29 ± 0.03	0.41 ± 0.03*
Net energy expenditure (kJ)	1,244 ± 152	781 ± 85*
Net energy expenditure/ ME intake (%)	51.7 ± 2.9	34.1 ± 2.5*
Insulin (ng/ml)	2.48 ± 0.23	2.55 ± 0.21
Glucose (mg/dl)	178 ± 6	202 ± 6*
HOMA index	25.3 ± 1.3	29.6 ± 1.1*
NEFA (mmol/l)	0.051 ± 0.011	0.061 ± 0.012

Data are means ± SE of four different rats. HOMA index = (glucose [mg/dl] × insulin [mU/l])/405. ME, metabolizable energy. *$P < 0.05$ compared with controls.

TABLE 2
Citrate synthase activity and protein yield in IMF and SS skeletal muscle mitochondria at the end of semistarvation and after 7 days of refeeding

Semistarvation	Control	Restricted
Citrate synthase activity (μmol · min^{-1} · g^{-1} tissue)		
Homogenate	20.0 ± 0.65	16.7 ± 0.73*
IMF	6.46 ± 0.50	4.77 ± 0.46*
SS	2.39 ± 0.30	1.06 ± 0.16*
Citrate synthase specific activity (μmol · min^{-1} · mg^{-1} protein)		
IMF	3.20 ± 0.10	3.50 ± 0.10
SS	4.20 ± 0.10	3.80 ± 0.20
Protein yield (mg/g tissue)		
IMF	1.99 ± 0.19	1.32 ± 0.18*
SS	0.57 ± 0.03	0.28 ± 0.04*
Refeeding	**Control**	**Refed**
Citrate synthase activity (μmol · min^{-1} · g^{-1} tissue)		
Homogenate	16.2 ± 0.56	13.1 ± 0.63*
IMF	4.54 ± 0.32	4.11 ± 0.37
SS	1.52 ± 0.12	1.20 ± 0.08*
Citrate synthase specific activity (μmol · min^{-1} · mg^{-1} protein)		
IMF	2.95 ± 0.08	3.04 ± 0.10
SS	3.19 ± 0.06	3.34 ± 0.26
Protein yield (mg/g tissue)		
IMF	1.56 ± 0.12	1.35 ± 0.11
SS	0.49 ± 0.05	0.34 ± 0.02*

Data are means ± SE of six different experiments. *$P < 0.05$ compared with controls.

Mitochondrial SS and IMF protein mass from skeletal muscle at the end of semistarvation and refeeding was determined by using the mitochondrial marker enzyme citrate synthase. At the end of the semistarvation period, citrate synthase activity per gram tissue was found to be significantly lower in the food-restricted rats than in controls, both in muscle homogenate and in isolated SS and IMF mitochondria, whereas no differences were found in citrate synthase specific activity per milligram protein in SS and IMF mitochondria (Table 2). In addition, the yield of both SS and IMF mitochondria from the food-restricted rats was lower than that from control rats (Table 2), whereas recovery of citrate synthase activity was unchanged in the food-restricted rats compared with controls (Fig. 1*A*). After 1 week of refeeding, citrate synthase activity per gram tissue was also found to be lower in muscles from refed rats than those from controls, both in the homogenate and in isolated SS and IMF mitochondria (Table 2); this difference was statistically significant for the homogenate and for SS mitochondria but failed to reach statistical significance for IMF mitochondria. Citrate synthase specific activity per milligram protein in SS and IMF mitochondria was unchanged in refed rats compared with controls, whereas the yield of both SS and IMF mitochondria from refed animals was lower compared with controls (Table 2). This difference was more pronounced and statistically significant for SS mitochondria but failed to reach statistical significance for IMF mitochondria. Recovery of citrate synthase activity was unchanged in refed rats compared with controls (Fig. 1*B*).

Respiratory activities of SS and IMF skeletal muscle mitochondria were evaluated by using NAD, FAD, and lipid substrate (Table 3). At the end of semistarvation, state 3 respiratory activities of SS mitochondria were significantly lower in restricted rats than in controls with succinate and glutamate. During refeeding, state 3 respiratory activity of SS mitochondria was found to be lower in refed rats than in controls with glutamate and palmitoyl CoA as the substrate. In IMF mitochondria, by contrast, the respiratory activity tended to be higher in tissues from refed animals than from controls, with significant differences being reached when using succinate as substrate. No variation in state 4 respiratory activity was found in SS and IMF mitochondria at the end of semistarvation or during refeeding.

The results on mitochondrial proton leak, assessed by titration of steady-state respiration rate as a function of mitochondrial membrane potential in SS and IMF skeletal muscle mitochondria, are presented in Figs. 2 and 3. These titration curves are an indirect measurement of proton leak, because steady-state oxygen consumption rate (i.e., proton efflux rate) in nonphosphorylating mitochondria is equivalent to proton influx rate due to proton leak. Comparisons of these curves for mitochondria isolated from restricted and control rats show no difference in the basal proton leak of SS and IMF mitochondria (Fig. 2*A* and *B*). By contrast, palmitate-induced proton leak was lower in mitochondria from restricted rats than in controls, with this reduction being significant in IMF mitochondria (Fig. 2*C*) and marginal and nonsignificant for SS mitochondria (Fig. 2*D*). After 1 week of refeeding, however, both basal and palmitate-induced proton leak tended to be higher in mitochondria from refed rats than in those from controls,

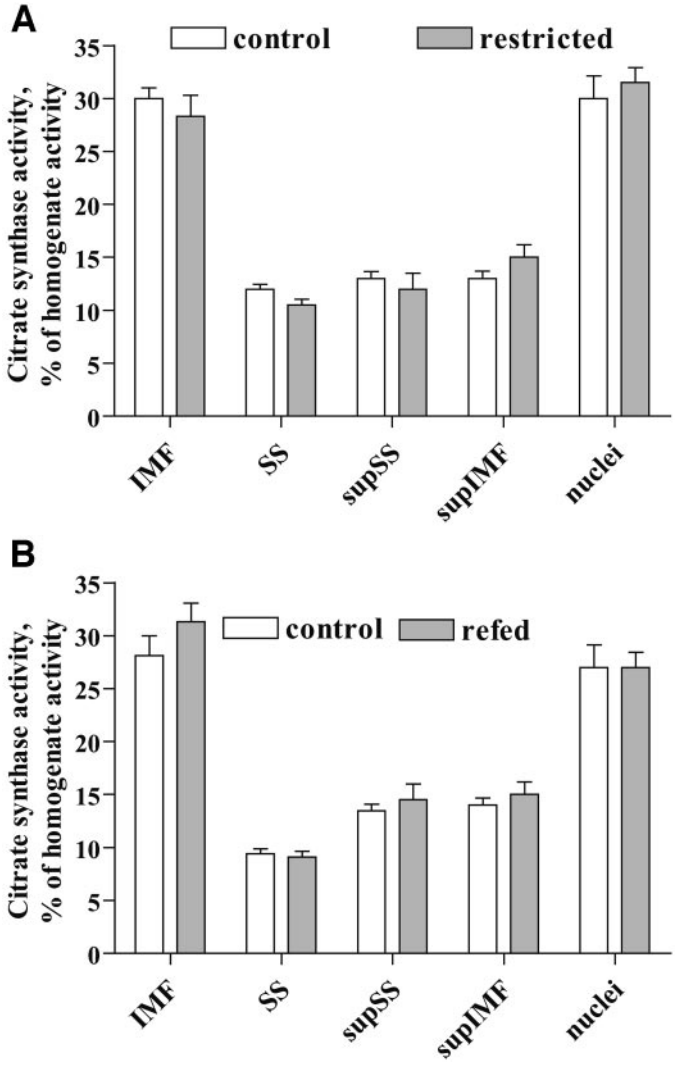

FIG. 1. Percent recovery of citrate synthase activity during mitochondrial isolation procedure at the end of semistarvation (*A*) and after 7 days of refeeding (*B*). Values are the means ± SE of six different experiments. supSS, SS supernatant; supIMF, IMF supernatant.

with differences being significantly different for basal proton leak in IMF mitochondria (Fig. 3*A*), and for palmitate-induced proton leak in both IMF and SS mitochondria (Fig. 3*C* and *D*).

The data on aconitase and SOD specific activity are shown in Table 4. At the end of semistarvation, no significant difference was found for aconitase activity in either IMF or SS mitochondria, but SOD activity was found to be significantly higher in both IMF and SS mitochondria from restricted rats than in those from controls. After 1 week of refeeding, SOD activity was also found to be significantly higher in SS mitochondria from refed rats than in controls, whereas aconitase activity was found to be significantly lower both in IMF and SS mitochondria from refed rats compared with controls.

UCP3 protein content in SS and IMF mitochondria, measured by Western blot analysis, was not found to be significantly different in restricted and refed animals compared with their respective controls (Table 4).

DISCUSSION

Evidence is presented here that diminished skeletal muscle mitochondrial mass and oxidative capacity, specifically in the SS compartment, could contribute to the high efficiency for catch-up fat. Furthermore, our findings of a lower aconitase activity in both SS and IMF muscle mitochondria from refed animals exhibiting an elevated HOMA index (and hence insulin resistance) underscore a potentially important link between diminished mitochondrial function and altered mitochondrial reactive oxygen species (ROS) production in the insulin resistance state of catch-up fat. To facilitate the discussion below, a summary of our main findings is presented schematically in Table 5.

Mitochondrial mass and oxidative capacity. Because >90% of cellular energy is produced during oxidative phosphorylation in mitochondria, changes in the mitochondrial protein mass (reflecting number, size, or both) or in oxidative capacity could exert profound effects on the efficiency of cellular metabolism. To assess changes in mitochondrial protein mass in response to semistarvation and refeeding, we used two approaches, namely *1*) by measuring the activity of a mitochondrial marker enzyme citrate synthase in skeletal muscle homogenates and in isolated SS and IMF mitochondria and *2*) by evaluating the mitochondrial yield (i.e., milligrams isolated protein per gram starting wet tissue) in each mitochondrial subpopulation. Independent of these two approaches used, we found that the mitochondrial mass was significantly reduced in both SS and IMF compartments at the end of semistarvation and that this reduction was more pronounced in SS than in IMF mitochondria (−56 vs. −26%). These differential changes in SS and IMF mitochondria in response to caloric restriction are even more marked after 1 week of refeeding, when the mitochondrial mass remained significantly lower than in controls in the SS compartment but not in the IMF compartment. The specificity of changes in SS mitochondria is also evidenced by our data on state 3 respiration rates, indicating a selective decrease in SS mitochondrial oxidative capacity. The reduction in state 3 respiration rates in the SS mitochondria both during semistarvation and refeeding contrasts with the lack of changes in this parameter in the IMF mitochondria whether during semistarvation or during refeeding. Taken together, our data indicating a continuum during semistarvation and early refeeding for diminished SS mitochondrial mass and oxidative capacity suggest that these quantitative and qualitative changes in the SS mitochondrial compartment could contribute importantly to the state of suppressed thermogenesis that favors catch-up fat during refeeding after caloric restriction.

Mitochondrial energetics and insulin resistance. The present finding of a persistent reduction in SS mitochondrial energetics during refeeding could also have major implications for the mechanism by which suppressed thermogenesis might lead to insulin resistance during catch-up fat. The fact that after 1 week of refeeding, the HOMA index, but not body fat or plasma NEFA, was higher in the refed animals than in controls suggests that the state of insulin resistance during refeeding precedes the development of excess adiposity or elevations in circulating NEFA. Using this same rat model, we previously reported that after 1 week of refeeding, i.e., at a time point when their body fat, plasma NEFA, and intramyocellular lipids had not exceeded those of controls, the refed rats showed higher plasma insulin after a glucose load (12) and a lower in vivo insulin-stimulated glucose utilization in skeletal muscle, as assessed by hyperinsulinemic-euglycemic clamp techniques (13). Taken together, these previous and present studies suggest that during weight recovery,

TABLE 3
State 3 and 4 respiratory activities of IMF and SS muscle mitochondria at the end of semistarvation and after 7 days of refeeding

	IMF		SS	
Semistarvation	Control	Restricted	Control	Restricted
Glutamate				
State 3	750 ± 50	746 ± 30	341 ± 20	256 ± 21*
State 4	47.4 ± 2.6	46.0 ± 1.3	33.8 ± 3.2	26.8 ± 2.3
RCR	16.0 ± 1.1	16.2 ± 0.6	10.3 ± 0.7	9.6 ± 0.1
Succinate				
State 3	791 ± 29	757 ± 16	388 ± 9	338 ± 13*
State 4	181 ± 6	169 ± 6	76.1 ± 2.1	77.3 ± 2.3
RCR	4.4 ± 0.1	4.5 ± 0.1	5.1 ± 0.2	4.4 ± 0.1*
Palmitoyl CoA				
State 3	339 ± 11	358 ± 22	141 ± 4	132 ± 7
State 4	33.5 ± 0.6	36.6 ± 1.2	29.8 ± 1.4	25.4 ± 2.1
RCR	10.1 ± 0.3	9.8 ± 0.6	4.7 ± 0.2	5.3 ± 0.7
Refeeding	Control	Refed	Control	Refed
Glutamate				
State 3	877 ± 19	883 ± 45	357 ± 21	263 ± 21*
State 4	49.4 ± 3.0	54.8 ± 1.4	32.5 ± 2.0	36.1 ± 1.4
RCR	18.1 ± 1.2	16.1 ± 1.4	11.0 ± 0.8	7.3 ± 0.3*
Succinate				
State 3	857 ± 22	982 ± 22*	418 ± 16	406 ± 25
State 4	177 ± 7	188 ± 2	86.8 ± 3.4	82.7 ± 4.4
RCR	4.8 ± 0.2	5.2 ± 0.1	4.8 ± 0.1	4.9 ± 0.2
Palmitoyl CoA				
State 3	359 ± 25	380 ± 21	154 ± 5	125 ± 6*
State 4	39.2 ± 1.8	42.3 ± 3.0	26.5 ± 0.9	28.6 ± 3.2
RCR	9.1 ± 0.3	9.0 ± 0.6	5.8 ± 0.4	4.6 ± 0.2

Data are means ± SE of six different experiments and are expressed as ng atoms oxygen · min^{-1} · mg^{-1} protein. RCR, respiratory control ratio. *$P < 0.05$ compared with controls.

the state of suppressed thermogenesis per se may have a direct impact on the development of skeletal muscle insulin resistance. Within this context, the quantitative and qualitative alterations in skeletal muscle SS mitochondria during refeeding have special significance for the pathogenesis of insulin resistance during catch-up fat. In fact, SS mitochondria provide energy for membrane-related processes, including signal transduction, ion exchange, substrate transport, and substrate activation (23), steps clearly relevant to insulin action, whereas the IMF mitochondria more directly support muscle contraction. A role for reduced SS mitochondrial energetics in the pathogenesis of skeletal muscle insulin resistance in obesity and in type 2 diabetes has recently been advanced, due to lower SS mitochondria and lower SS electron transport chain activity found in skeletal muscle from obese or diabetic patients than in nondiabetic lean volunteers (24). Thus, because of the potential importance of SS mitochondria for bioenergetic support of insulin signaling and insulin-mediated glucose transport in skeletal muscle, the possibility arises that the decreased mitochondrial energetics, specifically in the SS compartment, shown here during refeeding, may also play a role in the mechanism by which suppressed thermogenesis in skeletal muscle leads to insulin resistance during catch-up fat.

Proton leak, aconitase, and control of ROS production. We also examined whether mitochondrial uncoupling via proton leak mechanisms might also be reduced

TABLE 4
Aconitase and SOD specific activity and UCP3 protein content in IMF and SS skeletal muscle mitochondria at the end of semistarvation and after 7 days of refeeding

	IMF		SS	
Semistarvation	Control	Restricted	Control	Restricted
Aconitase (mU/mg protein)	46.88 ± 2.04	52.35 ± 2.81	88.33 ± 6.01	78.67 ± 4.38
SOD (units/mg protein)	50.25 ± 3.47	61.88 ± 3.66*	38.68 ± 4.25	53.85 ± 1.18*
UCP3 protein content (arbitrary units/mg protein)	38 ± 5	52 ± 5	22 ± 9	29 ± 6
Refeeding	Control	Refed	Control	Refed
Aconitase (mU/mg protein)	71.98 ± 8.72	48.42 ± 2.28*	103.50 ± 4.07	87.43 ± 4.96*
SOD (units/mg protein)	23.42 ± 1.41	22.55 ± 2.18	23.25 ± 1.83	31.38 ± 2.11*
UCP3 protein content (arbitrary units/mg protein)	45 ± 2	50 ± 3	28 ± 4	20 ± 7

Data are means ± SE of six different experiments. *$P < 0.05$ compared with controls.

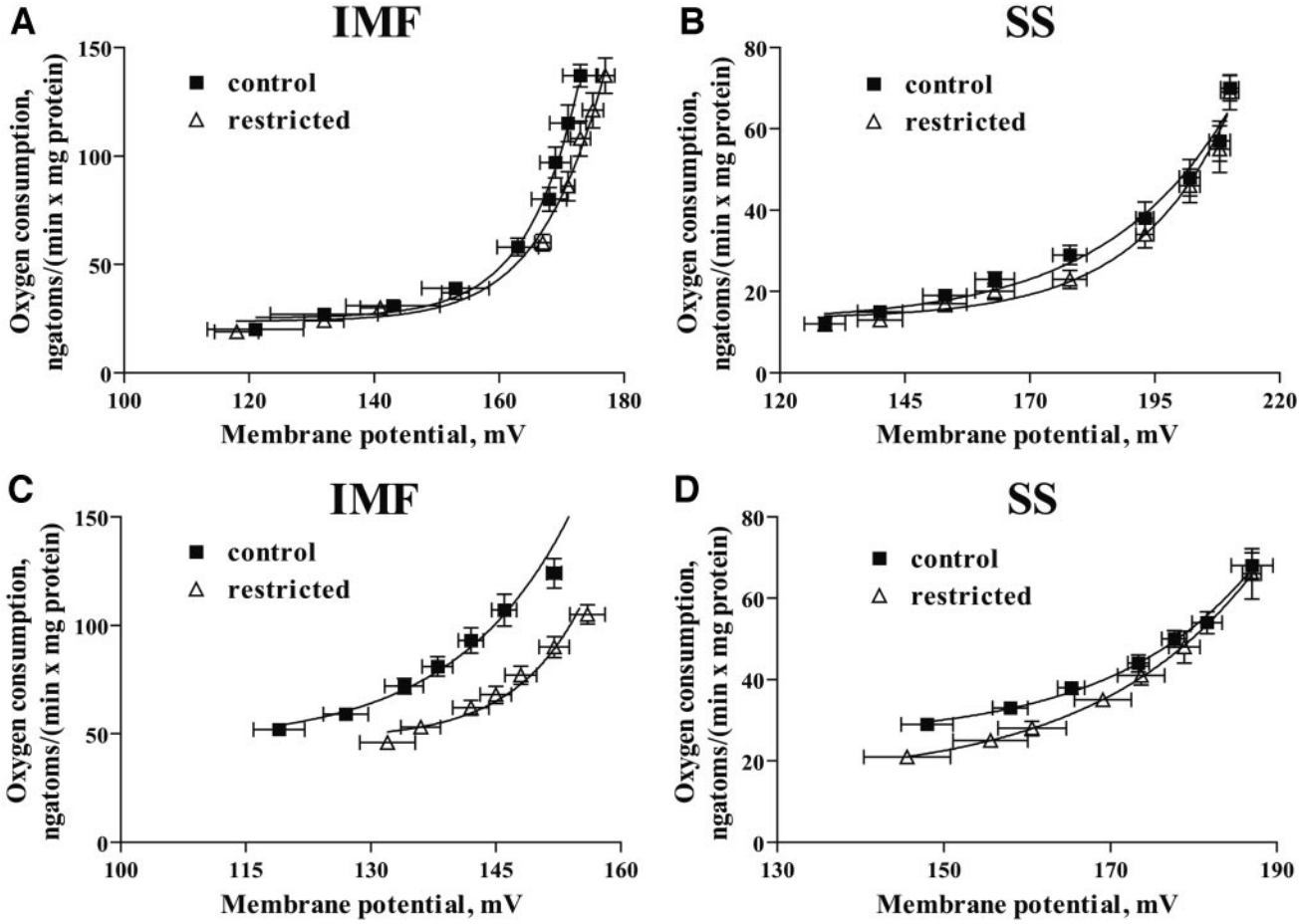

FIG. 2. Kinetics of basal (*A* and *B*) and palmitate-induced (*C* and *D*) proton leak in IMF (*A* and *C*) and SS (*B* and *D*) skeletal muscle mitochondria at the end of semistarvation. Values are the means ± SE of six different experiments. Nonlinear regression curve fits showed that palmitate-induced proton leak was significantly ($P < 0.05$) lower in IMF mitochondria from restricted rats compared with controls, whereas no significant difference was found in palmitate-induced proton leak in SS mitochondria from restricted rats compared with controls and in basal proton leak in IMF and SS mitochondria from restricted rats compared with controls.

in SS and IMF muscle mitochondria by measuring basal and fatty-acid dependent proton leak. The results show that basal proton leak and/or palmitate-induced proton leak were higher in both SS and IMF muscle mitochondria from refed rats than those from controls. These findings are clearly not in accord with a role for altered skeletal muscle proton leak in the mechanisms by which thermogenesis is suppressed. In addition, no change in UCP3 in SS or IMF muscle mitochondria was found during semistarvation or refeeding, confirming the dissociation between UCP3 and the regulation of mitochondrial proton leak (25,26).

The present data on proton leak are much more consistent with an increasingly advocated role for proton leak in the control of mitochondrial ROS. These are mainly produced during the resting state of the respiratory chain, when the proton gradient ($\Delta\mu H^+$) is elevated (27), thereby leading to an increased probability for electrons to react directly with dioxygen and to form superoxide and related ROS (28). Because ROS production is low when $\Delta\mu H^+$ is reduced, it has been hypothesized that a mild uncoupling of oxidative phosphorylation during state 4 respiration, by dissipating the proton gradient, would prevent ROS accumulation within the mitochondria (29). Therefore, an important physiological implication of the elevated basal and/or palmitate-induced proton leak in SS and IMF muscle mitochondria during refeeding could be to counter an

TABLE 5
Summary of results about direction of changes relative to controls at the end of semistarvation and after 7 days of refeeding

	Semistarvation		1 week refeeding	
Mitochondrial compartment	IMF	SS	IMF	SS
Mitochondrial mass	⇓	⇓ ⇓	↓	⇓ ⇓
Maximal oxidative capacity				
State 3				
Succinate	–	⇓	↑	⇓
Glutamate	–	⇓	↑	⇓
Palmitoyl CoA	–	⇓	↑	↓
State 4	–	–	–	–
Proton leak				
Basal	–	–	⇑	↑
Palmitate-induced	⇓	–	⇑	⇑
UCP3	–	–	–	–
Oxidative damage/ defense				
Aconitase	–	–	⇓	⇓
SOD	⇑	⇑	–	⇑

Double arrows indicate significant difference; regular arrows indicate tendency (with no significant differences); – indicates no significant difference and no tendency of a difference.

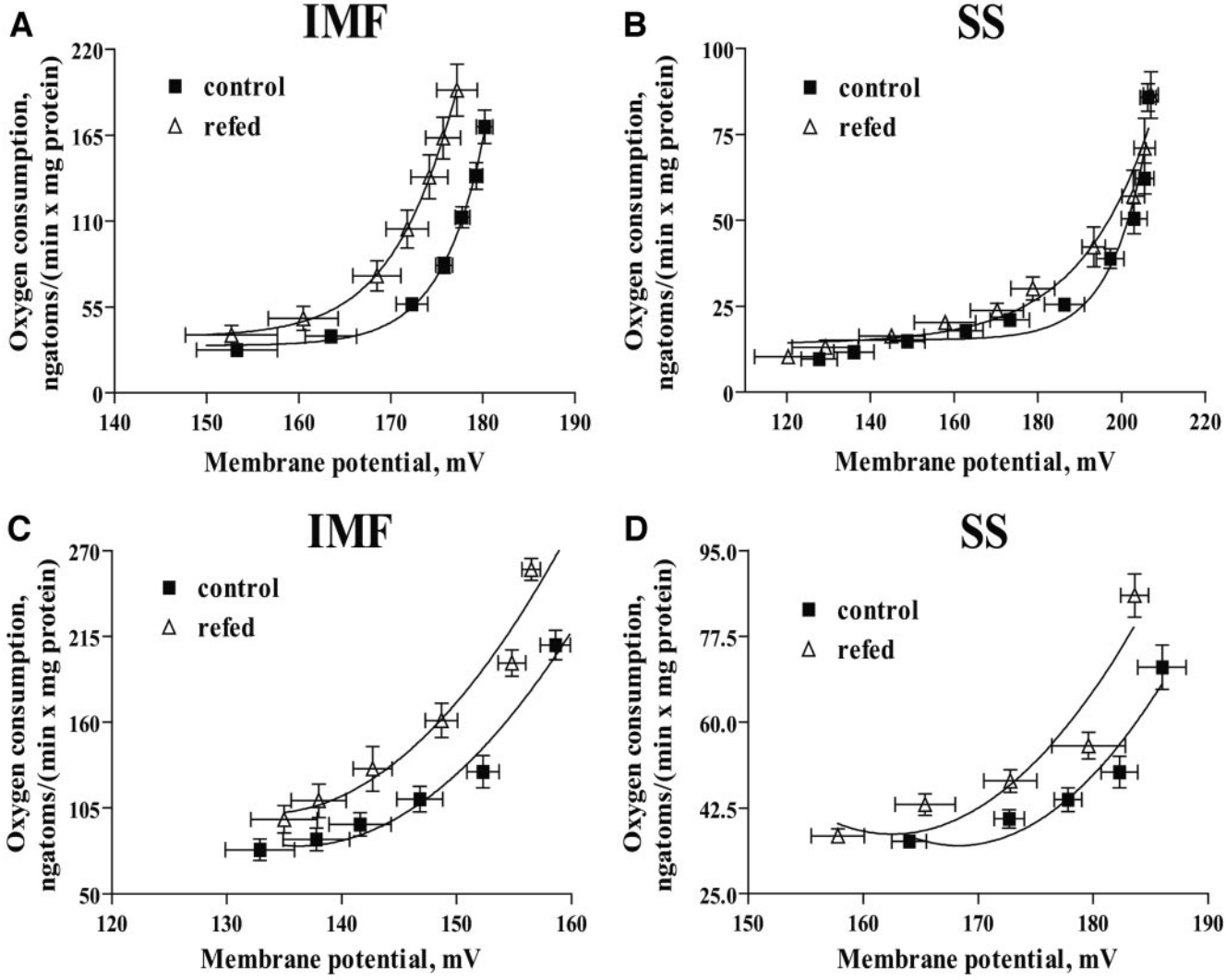

FIG. 3. Kinetics of basal (*A* and *B*) and palmitate-induced (*C* and *D*) proton leak in IMF (*A* and *C*) and SS (*B* and *D*) skeletal muscle mitochondria after 7 days of refeeding. Values are the means ± SE of six different experiments. Nonlinear regression curve fits showed that basal proton leak was significantly ($P < 0.05$) higher in IMF mitochondria from refed rats compared with controls, whereas there was no significant difference in SS mitochondria from refed rats compared with controls. In addition, palmitate-induced proton leak was significantly ($P < 0.05$) higher in IMF and SS mitochondria from refed rats compared with controls.

increased ROS production, especially at rest when energy turnover in skeletal muscle is low. This contention that mitochondrial ROS production is increased in skeletal muscle during refeeding may draw support from our findings *1*) that both SS and IMF muscle mitochondria from the refed animals also show a lower aconitase activity (whose inactivation is an index of ROS production) and *2*) that the SS mitochondrial compartment also show an increase in SOD activity, thereby suggesting an increase in antioxidant defenses.

Thus, our data suggest that the dynamic phase of catch-up fat during refeeding is a state of increased ROS levels in skeletal muscle despite the increased ROS scavenging. To what extent an increased ROS levels in skeletal muscle might be causative or consequential to the state of insulin resistance during refeeding is not known. However, the integration of data from our present and previous studies (12,13) underscores a potential link between diminished SS mitochondrial energetics, altered mitochondrial ROS levels, and insulin resistance in rats showing catch-up fat as a result of suppressed thermogenesis.

In conclusion, the present studies suggest that diminished skeletal muscle mitochondrial mass and oxidative capacity, specifically in the SS compartment, may contribute to the high efficiency of body fat recovery after caloric restriction. Given the important role that SS mitochondria have for bioenergetic support of signal transduction and substrate transport and hence for insulin action, these findings may have particular relevance in the mechanism by which suppressed thermogenesis in skeletal muscle leads to insulin resistance during catch-up fat, with implications for the physio(patho)logy of catch-up growth, weight fluctuations, and frequent "yo-yo" dieting.

ACKNOWLEDGMENTS

This work was supported by the Italian Ministry of Education, University and Research Grant COFIN 2003 and by the Swiss National Research Foundation Grant 3200B0-10215.

We thank Dr. Emilia De Santis for skillful management of the animal house.

REFERENCES

1. Keys A, Brozek J, Henschel A, Mickelson O, Taylor HL: *The Biology of Human Starvation.* Minneapolis, MN, University of Minnesota Press, 1950
2. Dulloo AG, Girardier L: 24h energy expenditure several months after weight loss in the underfed rat: evidence for a chronic increase in whole-body metabolic efficiency. *Int J Obes* 17:115–123, 1993
3. Dulloo AG, Jacquet J: Adaptive reduction in basal metabolic rate in response to food deprivation in humans: a role for feedback signal from the fat stores. *Am J Clin Nutr* 68:599–606, 1998
4. Miller DS, Wise A: The energetics of 'catch-up' growth. *Nutr Metab* 20:125–134, 1976
5. Boyle PC, Storlien LH, Keesey RE: Increased efficiency of food utilization following weight loss. *Physiol Behav* 21:261–264, 1978
6. Boyle PC, Storlien LH, Harper AE, Keesey RE: Oxygen consumption and locomotor activity during restricted feeding and realimentation. *Am J Physiol* 241:R392–R397, 1981
7. Hill JO, Fried SK, Digirolamo M: Effects of fasting and restricted refeeding on utilization of ingested energy in rats. *Am J Physiol* 247:R318–R327, 1984
8. Dulloo AG, Girardier L: Adaptive changes in energy expenditure during refeeding following low calorie intake: evidence for a specific metabolic component favoring fat storage. *Am J Clin Nutr* 52:415–420, 1990
9. Evans SA, Messina MM, Knight WD, Parsons AD, Overton JM: Long-Evans and Sprague-Dawley rats exhibit divergent responses to refeeding after caloric restriction. *Am J Physiol Regul Integr Comp Physiol* 288:R1468–R1476, 2005
10. Dulloo AG, Jacquet J: An adipose-specific control of thermogenesis in body weight regulation. *Int J Obes Relat Metab Disord* 25 (Suppl. 5): S22–S29, 2001
11. Dulloo AG, Jacquet J, Montani JP: Pathways from weight fluctuation to metabolic disease: focus on maladaptive thermogenesis during catch-up fat. *Int J Obes* 26 (Suppl. 2):S46–S57, 2002
12. Crescenzo R, Samec S, Antic V, Rohner-Jeanrenaud F, Seydoux J, Montani JP, Dulloo AG: A role for suppressed thermogenesis favoring catch-up fat in the pathophysiology of catch-up growth. *Diabetes* 52:1090–1097, 2003
13. Cettour-Rose P, Samec S, Russell AP, Summermatter S, Mainieri D, Carrillo-Theander C, Montani JP, Seydoux J, Rohner-Jeanrenaud F, Dulloo AG: Redistribution of glucose from skeletal muscle to adipose tissue during catch-up fat: a link between catch-up growth and later metabolic syndrome. *Diabetes* 54:751–756, 2005
14. Iossa S, Mollica MP, Lionetti L, Crescenzo R, Botta M, Liverini G: Skeletal muscle oxidative capacity in rats fed high-fat diet. *Int J Obes* 26:65–72, 2002
15. Cadenas S, Buckingham JA, Samec S, Seydoux J, Din N, Dulloo AG, Brand MD: UCP2 and UCP3 rise in starved skeletal muscle but mitochondrial proton conductance is unchanged. *FEBS Lett* 462:257–260, 1999
16. Iossa S, Lionetti L, Mollica MP, Crescenzo R, Botta M, Samec S, Dulloo AG, Liverini G: Differences in proton leak kinetics, but not in UCP3 protein content, in SS and intermyofibrillar skeletal muscle mitochondria from fed and fasted rats. *FEBS Lett* 505:53–56, 2001
17. Nedergaard J: The relationship between extramitochondrial Ca2+ concentration, respiratory rate, and membrane potential in mitochondria from brown adipose tissue of the rat. *Eur J Biochem* 133:185–191, 1983
18. Iossa S, Mollica MP, Lionetti L, Crescenzo R, Tasso R, Liverini G: A possible link between skeletal muscle mitochondrial efficiency and age-induced insulin resistance. *Diabetes* 53:2861–2866, 2004
19. Srere PA: Citrate synthase. *Methods Enzymol* 13:3–5, 1969
20. Gardner PR: Aconitase: sensitive target and measure of superoxide. *Methods Enzymol* 349:9–16, 2002
21. Flohè L, Otting F: Superoxide dismutase assay. *Methods Enzymol* 105:93–104, 1984
22. Matthews DR, Hosker JP, Rudenski AS, Naylor BA, Treacher DF, Turner RC: Homeostasis model assessment: insulin resistance and beta-cell function from fasting plasma glucose and insulin concentrations in man. *Diabetologia* 28:412–419, 1985
23. Hood D: Plasticity in skeletal, cardiac, and smooth muscle: contractile activity-induced mitochondrial biogenesis in skeletal muscle. *J Appl Physiol* 90:1137–1157, 2001
24. Ritov VB, Menshikova EV, He J, Ferrell RE, Goodpaster BH, Kelley DE: Deficiency of SS mitochondria in obesity and type 2 diabetes. *Diabetes* 54:8–14, 2005
25. Harper ME, Dent RM, Bezaire V, Antoniou A, Gauthier A, Monemdjou S, McPherson R: UCP3 and its putative function: consistencies and controversies. *Biochem Soc Trans* 29:768–773, 2001
26. Dulloo AG, Seydoux J, Jacquet J: Adaptive thermogenesis and uncoupling proteins: a reappraisal of their roles in fat metabolism and energy balance. *Physiol Behav* 83:587–602, 2004
27. Korshunov SS, Skulachev VP, Starkov AA: High protonic potential actuates a mechanism of production of reactive oxygen species in mitochondria. *FEBS Lett* 416:15–18, 1997
28. Papa S, Skulachev VP: Reactive oxygen species, mitochondria, apoptosis and aging. *Mol Cell Biochem* 174:305–319, 1997
29. Miwa S, Brand MD: Mitochondrial matrix reactive oxygen species production is very sensitive to mild uncoupling (Review). *Biochem Soc Trans* 31:1300–1301, 2003